Original Article

Effects of pore size and implant volume of porous hydroxyapatite/collagen (HAp/Col) on bone formation in a rabbit bone defect model

Akio Tsuchiya[1,2], Shinichi Sotome[1], Yoshinori Asou[1], Masanori Kikuchi[3], Yoshihisa Koyama[4], Tetsuro Ogawa[5], Junzo Tanaka[6] and Kenichi Shinomiya[1,2,7]

1) Section of Orthopaedic and Spinal Surgery, Tokyo Medical and Dental University, Graduate School, 1-5-45 Yushima, Bunkyo-ku, Tokyo 113-8519, Japan
2) 21st Century Center of Excellence Program for Frontier Research on Molecular Destruction and Reconstruction of Tooth and Bone, Tokyo Medical and Dental University, 1-5-45 Yushima, Bunkyo-ku, Tokyo 113-8519, Japan
3) Biomaterial Center, National Institute for Materials Science, 1-1 Namiki, Tsukuba, Ibaraki 305-0044, Japan
4) Institute of Biomaterials and Bioengineering, Tokyo Medical and Dental University, 2-3-10 Kanda-Surugadai, Chiyoda-ku, Tokyo 101-0062, Japan
5) PENTAX Corporation, 2-36-9 Maeno-cho, Itabashi-ku, Tokyo 174-8639, Japan
6) Department of Metallurgy and Ceramics Science, Tokyo Institute of Technology, Graduate School, 2-12-1, S7-5, Ookayama, Meguro-ku, Tokyo 152-8550, Japan
7) Advanced Bone and Joint Science, Tokyo Medical and Dental University, 1-5-45 Yushima, Bunkyo-ku, Tokyo 113-8519, Japan

A porous hydroxyapatite/collagen composite (HAp/Col) was developed that consists of hydroxyapatite nanocrystals and atelocollagen. In this study, cylindrical (diameter: 5 mm, height: 3 mm) porous HAp/Col implants with different pore sizes (diameter: 160 or 290 μm) were prepared, and the influences of pore size and implanted volume were evaluated using a rabbit bone defect model. In the implant groups, one or three (diameter: 5 mm, total height: 9 mm) implants were transplanted into bone holes created in the anteromedial site of the proximal tibiae, while a group without implantation was used as a control. Histological observation revealed that at two weeks after implantation, bone formation was initiated not only from the periosteum but in regions where the implants bordered on bone marrow. At four weeks, bone formation expanded from the marrow cavity side into the center of the implants, particularly in those implants with large pores. At twelve weeks, four implant groups showed repair of cortical defects and implant absorption, which was thought to be the result of natural bone remodeling mechanisms. The control group showed bone formation developed from the periosteum without bone induction in the marrow cavity, and at four weeks, the bone hole was almost healed. pQCT analysis revealed that the expansion rates of bone tissue were higher in the large-pore implant groups than in the small-pore groups. These data demonstrate the osteoconductivity of porous HAp/Col and the importance of its porous structure.

Key Words: Hydroxyapatite/collagen composite (HAp/Col); Porous structure; Nanocomposite; Bone repair; Bioabsorbability

Introduction

Since the sintering method of hydroxyapatite preparation was devised, sintered hydroxyapatite has been applied as a biocompatible and osteoconductive bone filler.[1-4] Due to its osteoconductivity, bone is formed around the implanted hydroxyapatite when implanted into a bone defect. Although the sintered hydroxyapatite is osteoconductive and biocompatible, it is scarcely absorbed and therefore remains in the body throughout the patient's life.

In contrast, hydroxyapatite/collagen (HAp/Col) nanocomposite is a bioabsorbable material.[5-9] HAp/Col nanocomposite fibers are synthesized from type I atelocollagen, $Ca(OH)_2$, and H_3PO_4, and are composed of collagen fibers and hydroxyapatite nanocrystals. The structure of HAp/Col nanocomposites is similar to that of natural bone; the hydroxyapatite needle crystals in the HAp/Col nanocomposite are aligned along the collagen fibers in the direction of the c-axis of the crystals, and their length is about 50 nm.[5,6] At the beginning of the development of HAp/Col bone filler, implants were developed as a dense-body formed by consolidation using the cold isostatic pressure method.[5] When implanted in a bone defect, bone formation was induced around the HAp/Col implant, and the implant was concurrently absorbed by osteoclast-like multi-nucleated cells. However, since cells could not penetrate into the dense implant, these responses occurred only at the periphery.

To solve the abovementioned problems, a porous HAp/Col material was developed.[11,12] The most distinctive characteristics of the porous HAp/Col are its sponge-like elasticity and superior handling in surgery, whereas most porous bone fillers which have already been developed and are in widespread clinical use are brittle.

The purpose of this study was to evaluate the influences of pore size and the implanted volume of porous HAp/Col on bone formation and absorption of the implants. In this study, porous HAp/Col constructs with different pore sizes were evaluated using a rabbit tibia bone defect model, and the influences of implant volume were also examined.

Materials and Methods

Preparation of porous HAp/Col

HAp/Col nanocomposite fibers were synthesized from atelocollagen derived from porcine skin, $Ca(OH)_2$, and H_3PO_4 using a coprecipitation method according to a previous report by Kikuchi et al.[5] Briefly, atelocollagen (Nitta Gelatin Co., Japan) was dissolved in H_3PO_4 solution. Both the dissolved collagen and a $Ca(OH)_2$ suspension were placed in a water bath that was thermally stabilized at 40 °C, while controlling the speed of each instillation in order to keep the pH at 9.0. The starting materials were prepared such that the composition of the final HAp/Col nanocomposites would be at an 80/20 weight ratio. The HAp/Col fibers were obtained as precipitates, and were lyophilized for preparation of porous HAp/Col implants. Porous HAp/Col implants were produced as follows: The HAp/Col fibers (1 g) were homogenized with 6.5 ml of phosphate buffered saline and alkalized with 50 μl of 1 M sodium hydroxide solution. The solution was mixed with 1.5 ml of 0.6% collagen solution dissolved in phosphoric acid (pH 2.0). The mixture at pH 7.0 was infused into a mold. To initiate gelation of the collagen as a binder, the mold containing the mixture was incubated at 37 °C for two hours. Then, the gelated HAp/Col gel was frozen, and the liquid within the mixture formed ice crystals in the HAp/Col gel. The spaces occupied by the ice crystals were converted to pores by subsequent lyophilization. The pore size of the porous HAp/Col was controlled by the freezing conditions. Rapid freezing of the gel resulted in small ice crystals, and thus, small pores. In this study, HAp/Col was prepared with large or small pores by freezing the HAp/Col gels at -30 °C or -80 °C, respectively. The lyophilized porous HAp/Col constructs were crosslinked by thermal dehydration at 140 °C under vacuum and then cut into a cylindrical shape (diameter: 5 mm, thickness: 3 mm) and sterilized by irradiation.

The porosity of the implants was set at 95%, which was calculated from the compositional ratios of HAp/Col fibers and water. The surface of the porous HAp/Col was observed by scanning electron microscopy (Hitachi S4200 FESEM, HITACHI, Tokyo, Japan). The average diameters of the pores were measured by the intercept method,[12,13] and the interconnected micropore size distribution was measured by mercury injection porosimetry.[14]

Implantation of porous HAp/Col into bone defects

All animal procedures were performed in accordance with the guidelines of Tokyo Medical and Dental University for the care and use of laboratory animals. The porous HAp/Col implants were implanted into bone holes created in the tibiae of Japanese white rabbits (male, 2.5-3.0 kg). The rabbits were anesthetized

by intramuscular injection of medetomidine hydrochloride (0.5 mg/kg) and ketamine hydrochloride (25 mg/kg), and anesthesia was maintained at 30 minute intervals by intramuscular injection of half doses of the above. Under sterile conditions, an incision was made in the anterior aspect of the proximal tibia. The periosteum was detached before the bone hole was created. A full thickness unicortical and trabecular bone defect was excavated on the anteromedial aspect of the tibia at the level of the tibial tuberosity, using a trephine drill (ϕ5 mm) with continuous saline irrigation to prevent thermal necrosis of the margins. After the drilling, drilling debris and remnants of the bone marrow were removed by flushing with saline. Fifty-six rabbits were randomly distributed into three groups (Table 1). In Group 1, the bone defects were closed with a small-pore HAp/Col implant in the right tibia and with three small-pore implants in the left tibia, and the implants were adjusted until the surface of the cortical bone was flat (n = 4-6). In Group 2, the bone defects of the tibia were closed with a large-pore implant in the right tibia and three large-pore implants in the left tibia, by the same means as in Group 1 (n = 4-6). Consequently, the implant in the right tibia was placed separately from the posterior and lateral aspects of cortical bone, maintaining its original form. In contrast to the right tibia, the implants of the left tibia were squeezed into the void where the volume was the same as that of the right tibia and shallower than 9 mm.

Therefore, in the three-implant groups, deformities of the implants were inevitable, especially at sites attached to the posterior and lateral cortical bone. After implantation, the defects were covered with the periosteum and the skin was closed. In Group 3, the control group, the defects on both the left and right sides were left unfilled and were only covered with the periosteum.

The animals were euthanized at 1, 2, 4, 8, and 12 weeks in the implant groups and at 2 and 4 weeks in the control group, and the tibiae were harvested and fixed in 4% paraformaldehyde for subsequent analysis.

Soft X-ray observations

Radiographs of the harvested tibiae, except the control group, were taken after fixation was completed with a radiograph unit (SRO-M50; SOFRON, Tokyo, Japan) and radiograph films (Fuji CR; Fujifilm, Tokyo, Japan).

Peripheral Quantitative Computed Tomography (pQCT) analysis

The harvested tibiae were scanned with peripheral quantitative computer tomography (pQCT) (XCT Research SA+; Stratec Medizintecnik GmbH, Pforheim, Germany). Measurements were taken at the center of the implants (boxel size: 120 × 120 μm, slice thickness: 460 μm).

Statistical analyses were performed on the implant-groups using statistical software (Stat View, SAS Institute, Inc., USA) for lack of the sample number of the control group for the analyses. Overall differences among the factors were determined by repeated measures ANOVA with factors of the pore size and the time course as independent factors and the number of implants as a dependent factor. If the ANOVA was significant, differences between individual groups were estimated using the Tukey-Kramer multiple comparison test. Differences were considered statistically significant when the p value was < 0.05.

Histological evaluation

The tibiae fixed in 4% paraformaldehyde were decalcified in ethylenedimine tetra acetic acid (EDTA) solution, dehydrated in a series of gradient ethanol exchanges, and embedded in paraffin. Sections of 5 μm thickness were stained by hematoxylin-eosin (HE) stain, tartrate-resistant acid phosphatase (TRAP) stain, and observed with an optical microscope.

Table 1. Implantation groups.

	Group 1 (Small-pore)		Group 2 (Large-pore)		Group 3
	one implant (right)	three implants (left)	one implant (right)	three implants (left)	defect
1w	6	6	6	6	-
2w	6	6	6	6	4
4w	6	6	6	6	4
8w	4	4	4	4	-
12w	4	4	4	4	-

Results

Property of porous HAp/Col

The porosity of the porous HAp/Col was 95% in this study. SEM images of the structures of the porous HAp/Col are shown in Figures 1A and 1B. The average pore size, as analyzed by the intercept method, was found to be 163.6 ± 77.1 μm in the small-pore HAp/Col constructs and 287.5 ± 126.3 μm in the large-pore HAp/Col constructs. Figure 1C shows the distributions of interconnecting pore size. The diameters of the interconnections were narrowly distributed at 2-3 μm in the small-pore HAp/Col material, whereas those of the large-pore constructs ranged widely from 0.8 μm to 50-400 μm. The porous structure was more uniform in the small-pore HAp/Col than in the large-pore HAp/Col.

Soft X-ray observation

Radiological observation was performed using soft X-ray images. At one week after implantation, the boundaries of the cortical bone defects were clear, and callus formation could not be observed on the cortical bone defects. The implants were somewhat recognizable in the marrow cavities. At four weeks, the boundaries of the cortical bone defects were obscure, and there were no radiolucent areas between the cortical bone and the implants. Regardless of pore size, the densities of the implant sites increased. At eight weeks, the cortical bone defects were almost completely repaired, and in bone marrow cavities, the areas of density increase were reduced compared to those observed at four weeks in all groups. At twelve weeks, the densities in the bone marrow cavities decreased to the normal density in each group (Fig. 2).

These data indicate that massive bone formation was induced for the entire implant site at four weeks, and that the cortical bone defects were repaired at eight weeks. Thereafter, at twelve weeks, the surplus bone and the implant had been absorbed.

pQCT analysis

At one week after implantation, the densities of the implants increased at the intramedullary sides. The areas where the density increased were broader in the large-pore implants than in the small-pore implants. At two weeks, the densities of the implant sites increased over almost the entire area filled with the large-pore implants, while the densities of the implant sites of the small-pore implants increased mainly in the peripheral areas. At eight weeks, the cortical bone defects were nearly repaired in all the groups, whereas in the bone marrow cavities, the densities were reduced. At twelve weeks, the repair and remodeling of the transplanted sites of all the implant groups was complete (Fig. 3A).

Bone tissue with a density of 690 mg/cm^3 and above is considered to be mature cortical bone.[15] In the implant groups, areas with a density of 690 mg/cm^3 and above were seen not only at the healing cortical defect, but also at the implant site in the marrow cavity (Fig. 3A). These areas were quantified in Fig. 3B. Although differences among the groups were obscure because intrinsic cortical bone could not be separated clearly and was included in all the data as a baseline, statistical differences were found between the one- and three-implant groups ($p < 0.05$), and the areas increased statistically at four weeks ($p < 0.05$). There was interaction between the number of implants and the time course. The peak of the large-pore implant
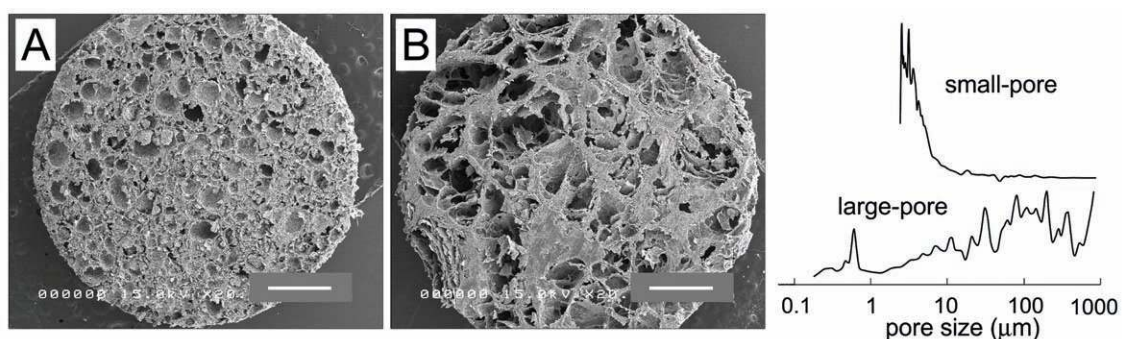
Fig. 1. Properties of porous HAp/Col. Scanning electron microscope images of the porous HAp/Col nanocomposites (A: small-pore construct, B: large-pore construct). Scale bar indicates 1 mm. Distributions of the pore sizes of the porous HAp/Col as measured by mercury injection porosimetry (C).
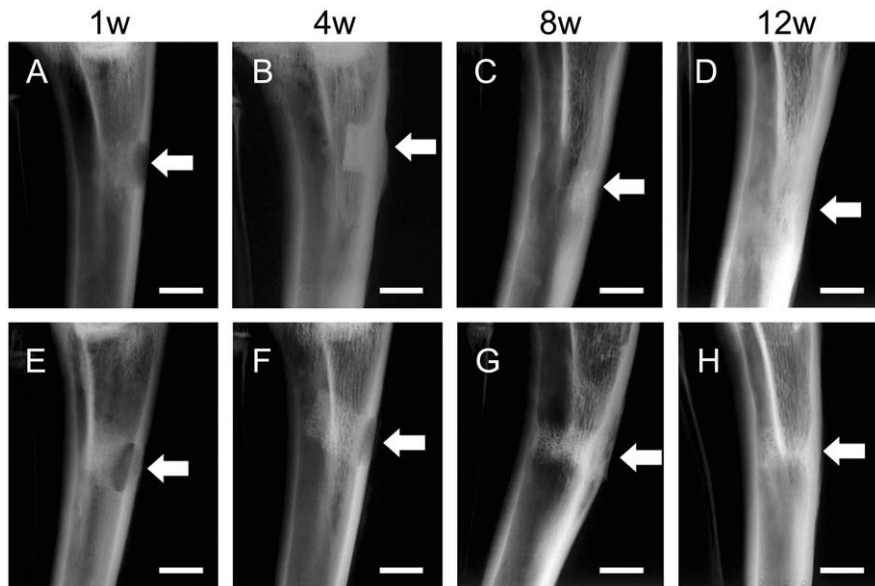
Fig. 2. Soft X-ray photographs of the tibiae implanted with the porous HAp/Col implants. Arrows indicate the implant site. The cortical bone defects were repaired at eight weeks. (Implant: small-pore, one implant (A-D), large-pore, one implant (E-H), small-pore, three implants (I-L), large-pore, three implants (M-P)). Scale bar indicates 5 mm.
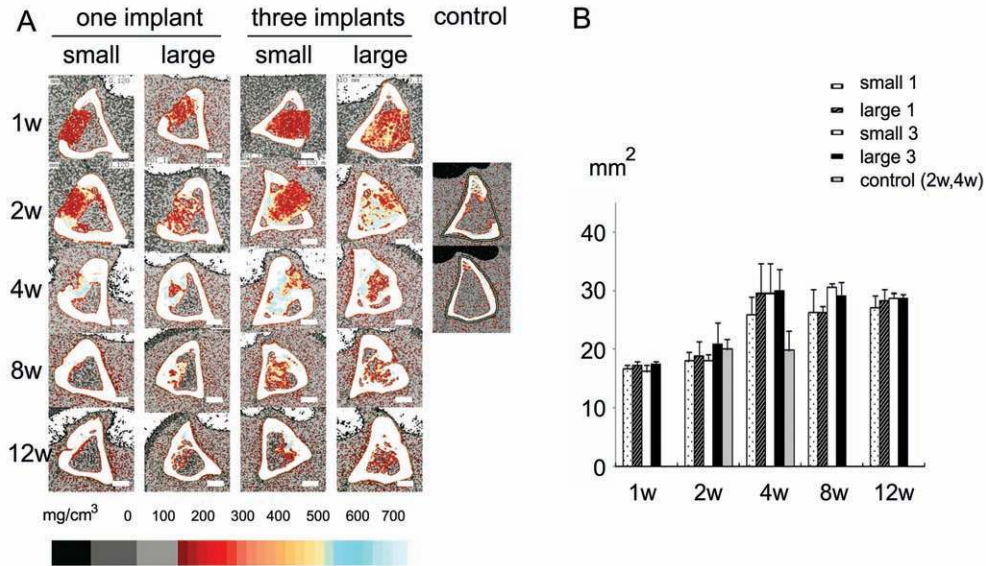
Fig. 3. pQCT analysis of porous HAp/Col implants. Representative images of pQCT scans. Scale bar indicates 2 mm (A). Quantitative analysis of the cortical bone areas where the density was 690 mg/cm^3 and above (B). *$p < 0.05$

group was at four weeks, whereas the areas of small-pore implant groups slightly increased at eight weeks after implantation. These data indicate that both bone conduction and remodeling at the marrow cavity occur at the defect guided by the large-pore implant earlier than near the small-pore implants, particularly when the implant volume is large.

Histological analysis

At one week after implantation, there was scarcely

any tissue invasion and no bone formation in the implants. Some implants in the single-implant group were slightly shifted towards the bone marrow cavity, and some of the three-implant groups slightly protruded outside of the marrow cavity, probably due to their elasticity. At two weeks, the bone formation in the implant groups had occurred in the area between the periosteum and the cortical bone around the bone hole, and in the peripheral areas of the implants following tissue invasion into the implants, especially on the bone marrow side (Fig. 4). In the control group, bone formation which had developed from the surrounding periosteum had progressed into the cortical bone defect area, although there was scarce bone formation in the bone marrow cavity. At four weeks in the implant groups, bone formations from the marrow cavities and the periosteum developed toward the cortical bone holes. In the large-pore implant groups, tissue invasion from the bone marrow side was more abundant than in the small-pore implant groups. In association with tissue invasion, more abundant bone formation occurred at the large-pore implant site than at the small-pore implant site in both the single implant groups and the three-implant groups. In the control group, the bone holes were almost closed by the bone tissue developed from the periosteum, with scarce bone formation in the bone marrow cavities (Fig. 5). At eight weeks in the implant groups, integration of bone tissue from the periosteum and from the marrow cavity was confirmed, the repaired cortical bone defects had matured, and absorption of the implants and the surplus bone in the marrow cavity had occurred more compared to that at four weeks. t at four weeks. At twelve weeks, implants and bone were absorbed further in the
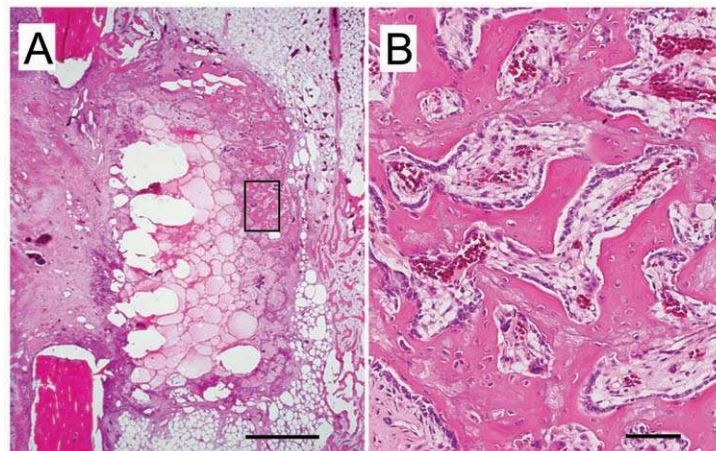
Fig. 4. Histological sections (H&E staining) of the defect site with a small-pore HAp/Col implant. (A, B: 2 weeks after implantation. B: magnified view of the rectangular area in A.)
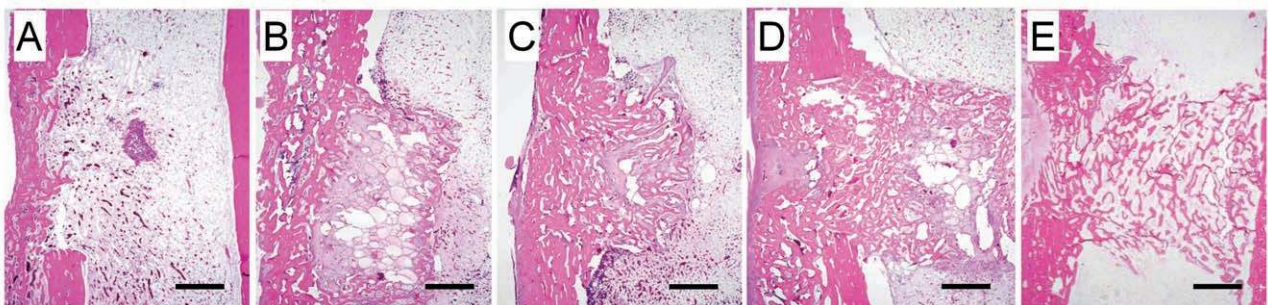
Fig. 5. Histological sections (H&E staining) of the transplanted sites at 4 weeks. A: defect. B: small-pore, one implant. C: large-pore, one implant. D: small-pore, three implants. E: large-pore, three implants. Scale bar, 1 mm.

bone marrow cavities (Fig. 6).

TRAP-positive multinucleated cells were observed attached to the newly formed bone and the implants from one week after implantation. TRAP positive cells were most abundant at two weeks, although the number of cells was not counted (Fig. 7).

Discussion

The porous structure of osteoconductive materials provides a greater area for bone formation, and bone formation occurs not only around the materials but also into their pores. Efficacious interpore connections allow cells to migrate into the materials, and blood vessels to grow into the materials, allowing for the nutrition,

oxygen, and excretion necessary for osteogenesis.[16] Therefore, we have developed a porous HAp/Col material.[10,11]

Critical factors of bone void fillers include their macrostructure, nanostructure, and chemical characteristics. With a focus on pore size and/or the interconnection of bone fillers, the effects of porous structure for bone formation have been investigated with sintered hydroxyapatite, β-tricalcium phosphate, and other calcium phosphate implants. Galois and Mainard implanted bone fillers with various pore sizes into bone defects and reported that the suitable pore size of calcium phosphate bone filler was approximated at 100-300 μm.[17] The importance of interconnection was also argued, and the favorable diameter of pore size was reported to range from 50 to 200 μm.[18-21] Thus,
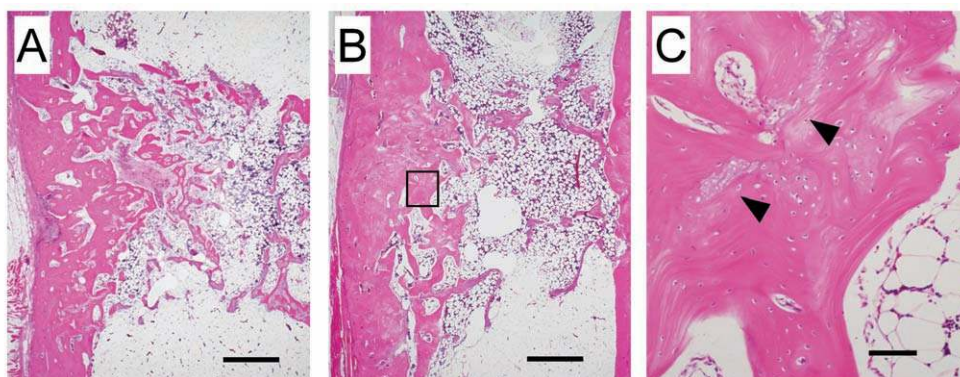
Fig. 6. Histological images (H&E staining) of the implant sites with three large-pore implants. A: 8 w, B, C: 12 w. C: magnified view of the rectangular area in B. At 12 w, the repaired cortical bone was matured, and the implants and the surplus bone were absorbed in bone marrow cavities. Arrow heads indicate residual implant.

HAp/Col   newly formed bone
TRAP(+) multinucleated cell
lining cells
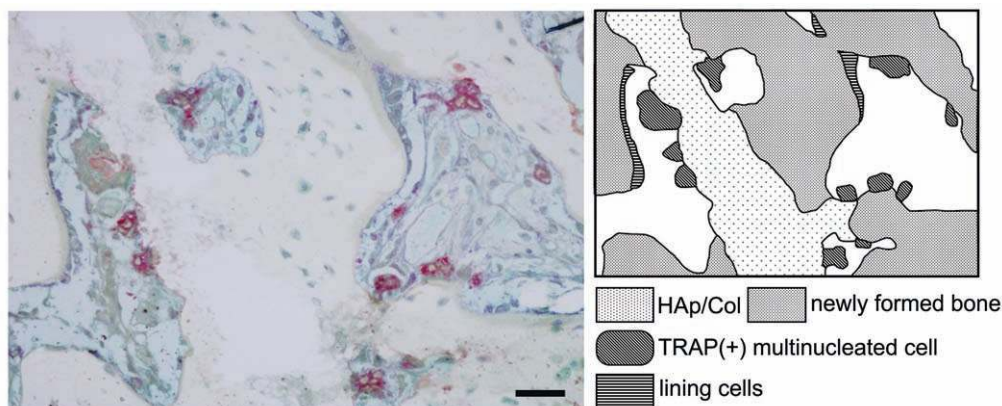
Fig. 7. TRAP stain images of the implant site with one large-pore implant at 2 w. Scale bar, 50 μm. TRAP positive multinucleated cells attach to the implant and conducted bone.

control of the pore structures of biomaterials is a vital technology for developing suitable scaffolds for bone formation.

Unlike existing sintered implants, for which the effects of porous structures have been well established as mentioned above, porous HAp/Col is elastic, and its compressive deformation and resultant deformation of the porous structure may be inevitable after its implantation. Consequently, information about the effects of porous structure obtained from past studies cannot be applied to porous HAp/Col. To explore the effects of pore size of porous HAp/Col, we compared two types of porous HAp/Col implants using a transplantation model in rabbit tibiae.

Although the experimental model used in this study is a transplantation model into a bone marrow cavity where the intrinsic trabecular bone scarcely exists, abundant bone formation was observed at the implant site of the porous HAp/Col, and thereafter, the bone tissue and the implant were absorbed. In association with the volumes of the transplanted implants, the bone formation amounts of the three-implant groups were larger than those of the single implant groups in the large-pore and small-pore groups, respectively. In contrast to the implant groups, scarce bone formation was observed in the bone marrow cavity of the control group. This demonstrates the osteoconductivity and absorbability of the porous HAp/Col implants. Comparing the large-pore and small-pore implants, the large-pore implants had a greater rate of tissue invasion than that of the small pore-implants, and more bone formation occurred at an earlier stage in the large-pore implant groups from the bone marrow side. This is thought to depend on the larger diameter of the interconnections of the large-pore implants and the larger number of interconnections as gateways for tissue invasion in the small-pore implants.

Although the cortical defect size in this study is not critical,[22] and therefore, the model is not considered to be suitable to evaluate the effectiveness in cortical bone healing, histological findings suggest that porous HAp/Col transplanted in the bone marrow cavity has a supportive effect on cortical bone healing. At cortical defect sites, regardless of group, bone formation mainly expanded from the periosteum around the defect, and the cortical defect was almost closed at four weeks. However, there was a distinct difference between the control and the implant groups. In the implant groups, bone formation in the implant site expanded forward into the cortical defect and was integrated into the bone from the periosteum, whereas there was scarce bone formation in the marrow cavity of the control. From these findings, porous HAp/Col implants transplanted in a bone marrow cavity would support cortical bone repair from inside the cavity, particularly where the bone formation capability of the periosteum is poor. This supportive effect would have been clear in this study if the periosteum had been removed.

In clinical orthopedic surgery, bone void fillers are mainly used to fill large cancellous bone defects caused by tumors, the harvest of autografts, severely displaced fractures, and so on. Therefore, osteoconductivity in the bone marrow cavity is the most important property of bone void fillers. This study demonstrated the use of large-pore HAp/Col as a bone void filler and indicated the beneficial properties of the porous structure.

Conclusion

Porous HAp/Col with distinctive elasticity and excellent handling characteristics was devised and tested using a rabbit bone defect model. The porous structure of the large-pore HAp/Col with sufficient interconnections facilitated tissue invasion and bone conduction compared to that of the small-pore HAp/Col. This indicates the importance of the porous structure, which allows for cell migration and vessel in-growth for prompt bone formation.

References

1. Denissen HW, de Groot K. Immediate dental root implants from synthetic dense calcium hydroxyapatite. J Prosthet Dent 1979;42:551-556.
2. LeGeros RZ. Properties of osteoconductive biomaterials: calcium phosphates. Clin Orthop 2002;395:81-98.
3. Bucholz RW. Nonallograft osteoconductive bone graft substitutes. Clin Orthop 2002;395:44-52.
4. Giannoudis RV, Dinopoulos H, Tsiridis E. Bone substitutes: An update. Injury Int J Care Injured 2005;36S:S20-S27.
5. Kikuchi M, Itoh S, Ichinose S *et al.* Self-organization mechanism in a bone-like hydroxyapatite/collagen nanocomposite synthesized *in vitro* and its biological reaction *in vivo*. Biomaterials 2001;22:1705-1711.
6. Rhee SH, Suetsugu Y, Tanaka J. Biomimetic configurational arrays of hydroxyapatite nanocrystals on bio-organics. Biomaterials 2001;22:2843-2847.

7. Itoh S, Kikuchi M, Takakuda K *et al*. The biocompatibility and osteoconductive activity of a novel hydroxyapatite/collagen composite biomaterial, and its function as a carrier of rhBMP-2. J Biomed Mater Res 2001;54:445-453.

8. Itoh S, Kikuchi M, Takakuda K *et al*. Implantation study of a novel hydroxyapatite/collagen (HAp/Col) composite into weight-bearing sites of dogs. J Biomed Mater Res 2002;63:507-515.

9. Itoh S, Kikuchi M, Koyama Y *et al*. Development of an artificial vertebral body using a novel biomaterial, hydroxyapatite/collagen composite. Biomaterials 2002;23:3919-3926.

10. Kikuchi M, Ikoma T, Syoji D *et al*. Porous body preparation of hydroxyapatite/collagen nanocomposites for bone tissue regeneration. Key Eng Mater 2004;254:561-564.

11. Sotome S, Orii H, Kikuchi M *et al*. *In vivo* evaluation of porous hydroxyapatite/collagen composite as a carrier of OP-1 in a rabbit PLF model. Key Eng Mater 2006;309-311:977-980.

12. Underwood E E, Colcord A R, Wangh W C *et al*. Ceramic Microstructures. Wiley and Sons 1966;p25-52.

13. Underwood E E. Quantitative Sterereology. Addison Wesley1970.
    Fullman R L. Trans AIME 1953;197:447-452.

14. Ritter H.L, Drake L C. Pore-size distribution in porous materials: Pressure porosimeter and determination of complete macropore-size distributions. Ind. Eng. Chem 1945;17:782-787.

15. Ferretti JL. Peripheral quantitative computed tomography for evaluating structural and mechanical properties of small bone. In: Yuehuei HA, Robert A D. Mechanical testing of bone and the bone-implant interface. Boca Raton FL: CRC press; 1999:385-405.

16. Karageorgiou V, Kaplan D. Porosity of 3D biomaterial scaffolds and osteogenesis. Biomaterials 2005;26:5474-5491.

17. Galois L, Mainard D. Bone ingrowth into two porous ceramics with different pore sizes: an experimental study. Acta Orthop Belg 2004;70:598-603.

18. Lu JX, Flautre B, Anselme K *et al*. Role of interconnections in porous bioceramics on bone recolonization *in vitro* and *in vivo*. J Mater Sci Mater Med 1999;10:111-120.

19. Flautre B, Descamps M, Delecourt C *et al*. Porous HA ceramic for bone replacement: role of the pores and interconnections - experimental study in the rabbit. J Mater Sci Mater Med 2001;12:679-682.

20. Tamai N, Myoui A, Tomita T *et al*. Novel hydroxyapatite ceramics with an interconnective porous structure exhibit superior osteoconduction *in vivo*. J Biomed Mater Res 2002;59:110-117.

21. Mastrogiacomo M, Scaglione S, Martinetti R *et al*. Role of scaffold internal structure on *in vivo* bone formation macroporous calcium phosphate bioceramics. Biomaterials 2006;27:3230-3237.

22. Aaboe M, Pinholt E M, Hjørting-Hansen E. Unicortical critical size defect of rabbit tibia is larger than 8 mm. J Craniofac Surg. 1994;5:201-203.